Camera Source Identification Using Discrete Cosine Transform Residue Features and Ensemble Classifier

Aniket Roy, Rajat Subhra Chakraborty
Department of Computer Science and Engineering
Indian Institute of Technology, Kharagpur
India
aniketroy@iitkgp.ac.in, rschakraborty@cse.iitkgp.ernet.in

Udaya Sameer and Ruchira Naskar
Department of Computer Science and Engineering
National Institute of Technology, Rourkela
India
{515cs1003, naskarr}@nitrkl.ac.in

Abstract

Machine Learning based model building and classification has proved to be extremely effective for the camera source identification problem. In this paper, we have proposed a camera source identification methodology, based on extraction of the Discrete Cosine Transform Residual *features, and subsequent* Random Forest *based ensemble classification with* AdaBoost. *We improve the classification accuracy by incorporating dimensionality reduction by* Principal Component Analysis. *Our experimental results on 10,507 images captured by ten cameras from the* Dresden Image Database *gives an average classification accuracy of 99.1%, and also show low overfitting trends when the constructed classifier is applied on a different image database.*

1. Introduction

Blind detection of camera source of an image is used to verify its origin and authenticity, and is considered a classic problem in digital forensics [1]. Most techniques for camera source identification aim to detect traces or artifacts that the source camera imparts onto the images, such as those resulting from the camera's demosaicing algorithms [2, 3], imaging sensor noise [4], lens-induced chromatic aberration [5], proprietary implementations of JPEG compression [6], etc. There are several quality metric, co-occurrence matrix and different feature based camera source identification schemes. Kharrazi et al. [1] used several *Image Quality Metric* (IQM) and *Non-Image Quality Metric* (Non-IQM) feature based classification technique for source camera identification. Choi et al. [7] proposed to use the lens radial distortion as a fingerprint to identify the source camera model. Efficient device identification from sensor dust patterns was proposed by Dirik et al. [8]. Bayram et al. [9] exploited the *Color Filter Array* (CFA) filter pattern for source camera identification. Local binary pattern based texture features have also been used for camera source identification [10].

Chen et al. [11] recently used co-occurrence matrix based features utilizing the rich model of the camera's demosaicing algorithm for efficient source camera identification, inspired by Fridrich et al.'s [12] work on rich models for steganalysis. Co-occurrence matrix based local features have been used by Marra et al. [13] for efficient camera model identification. Recently, in [14] Tuama et al. extracted higher order statistics from contaminated sensor noise by computing co-occurrence matrix based features for source camera identification, and further improved the performance by additionally incorporating color dependencies and conditional probability based features [15].

In this paper, we leverage certain camera-dependent artifacts introduced by JPEG compression in modern digital cameras to develop a classification based camera source detection methodology. Currently, JPEG is the most popular compression technique which uses *Discrete Cosine Transform* (DCT) based image compression with quantization [16]. Recently, Fridrich et al. [17] proposed a *Discrete Cosine Transform Residual* (DCTR) feature set utilizing first order statistics of the quantization noise residual obtained from the decompressed JPEG image, and applied

it for JPEG image steganalysis. **The main observation on which our technique is based is that the quantization tables used for the JPEG compression varies in different camera models, and hence can be considered an intrinsic property of different camera models. Therefore, JPEG compression incurs camera model dependent quantization noise in the image, and DCTR features can be used to identify the source camera through capturing the compression artifacts imposed by the camera model dependent quantization tables, as these features capture the first order statistics of quantization noise residuals. We found classification based on models built using these features to be highly accurate.** The following are our major contributions in the paper:

- To the best of our knowledge, this work reports the first application of DCTR features for high accuracy camera source identification.
- We explored several features and classification options, and based on our obtained experimental results, we have used a combination of *Principal Component Analysis* (PCA) based dimensionality reduction, and *AdaBoost* based ensemble classification with *Random Forest* (itself an ensemble classification technique) as the weak learner to achieve high accuracy levels. This combination of techniques was established to be the most suitable among other classification techniques through detailed experimentation (details in Section 3).
- Our proposed technique exhibits low overfitting trends, when the constructed classifier is applied on a different image database.

The rest of the paper is organized as follows. In Section 2, our proposed source camera identification framework is discussed in detail. Experimental results are given in Section 3, and finally conclusions are drawn in Section 4.

2. Source Camera Identification Framework

In this section, we present details of feature extraction, feature transformation and dimensionality reduction, and classification techniques based on the transformed features.

2.1. DCTR Feature Extraction

The steps for DCTR feature extraction from an image are as follows [17, 18]:

- The JPEG image is decompressed to spatial domain without quantizing the pixel values to $\{0, \cdots, 255\}$ to avoid any loss of information.
- The DCT basis patterns of size 8×8 are generated as

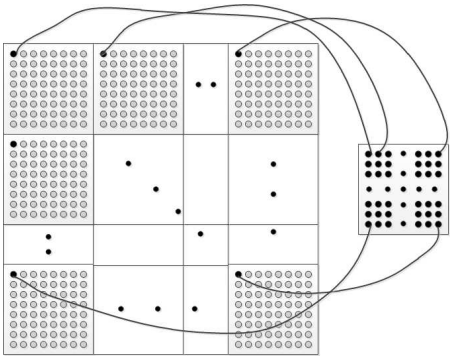

Figure 1. Subsampling procedure.

$\mathbf{B}^{(k,l)} = \left(B_{mn}^{(k,l)}\right), 0 \leq m, n \leq 7$:

$$B_{mn}^{(k,l)} = \frac{w_k w_l}{4} \cos \frac{\pi k \left(2m+1\right)}{16} \cos \frac{\pi l \left(2n+1\right)}{16} \tag{1}$$

where $w_0 = \frac{1}{\sqrt{2}}$, $w_i = 1$ for $i > 0$.

- The decompressed JPEG image $\mathbf{X}$ is convolved with each of the 64 DCT basis patterns $\mathbf{B}^{(k,l)}$, to generate a set of 64 undecimated DCT planes, each of which is denoted by $\mathbf{U}^{(k,l)}$ for (k,l)-th DCT basis pattern as:

$$\mathbf{U}^{(k,l)} = \mathbf{X} * \mathbf{B}^{(k,l)}, \qquad 0 \leq k, l \leq 7 \tag{2}$$

- According to the 64 DCT modes (a,b), $0 \leq a, b \leq 7$, corresponding to each DCT basis pattern in each 8×8 DCT block, the filtered undecimated DCT image $\mathbf{U}^{(k,l)}$ is sub-sampled by a step-size of 8 to get 64 sub-images $\mathbf{U}_{a,b}^{(k,l)}$, as shown in Fig. 1. The subsampling process enhances the diversity and effectiveness of the features, by accentuating the impact of the local features.
- For each sub-image $\mathbf{U}_{(a,b)}^{(k,l)}$, the histogram feature is extracted as:

$$\mathbf{h}_{a,b}^{(k,l)}\left(x\right) = \frac{1}{|\mathbf{U}_{a,b}^{(k,l)}|} \sum_{u \in \mathbf{U}_{a,b}^{(k,l)}} \left[Q_T\left(|u|/q\right) = x\right], \tag{3}$$

where Q_T is a quantizer with integer centroids $\{0, 1, \cdots, T\}$, q denotes the quantization step, and $[P]$ is the *Iverson Bracket*, which is equal to '0' when the statement P is false, and '1' when P is true. Here, the value of q is dependent on the JPEG quality factor [17], and the step size x for computing the histogram is 1.

- All the histogram features of the 64 sub-images $\mathbf{U}_{a,b}^{(k,l)}$ are merged and combined to obtain the histogram feature $\mathbf{h}^{(k,l)}$ of the filtered undecimated DCT image $\mathbf{U}^{(k,l)}$. This merging operation aids in dimensionality reduction because of statistical correlation between

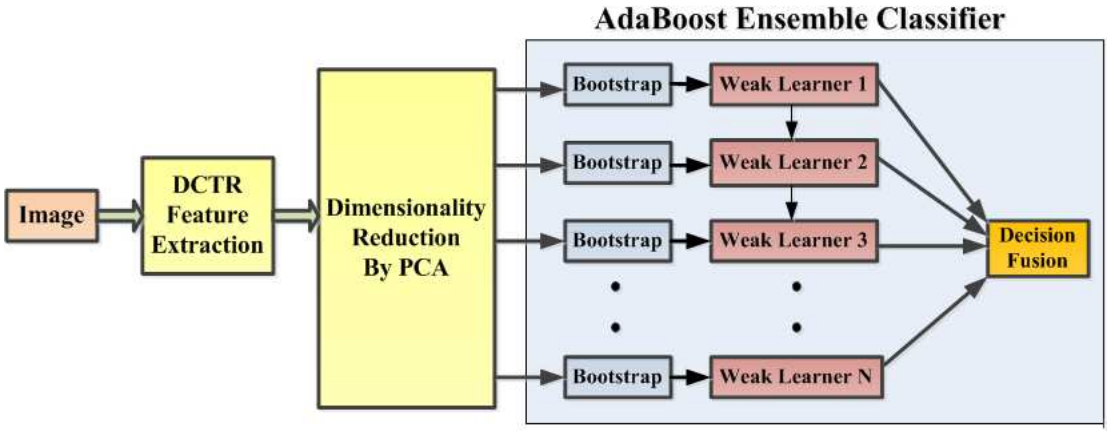

Figure 2. Flow chart of proposed Ensemble Classifier based training process. The blocks marked "Bootstrap" performs random sampling with replacement.

the histogram features of the sub-images, since images have similar statistical characteristics in symmetrical orientation. For example, since $\mathbf{U}^{(k,l)} = \mathbf{X} * \mathbf{B}^{(k,l)}$, and the sum of the elements of $\mathbf{B}^{(k,l)}$ is zero (these are DCT modes), for natural images $\mathbf{X}$, the distribution of $u \in \mathbf{U}^{(k,l)}_{(a,b)}$ will be approximately symmetrical, and centered at zero for all a, b.

- For each filtered image, sixty-four separate $(T+1)$-dimensional histogram feature sets could be obtained when the threshold for histogram is set to T. Then, these histogram features can be merged to form one histogram feature set with dimension $25\times(T+1)$ using symmetry properties [17]. Finally, for all the 64 sub-images total feature dimension would be $64\times25\times(T+1)$. Authors in [17] used DCTR feature dimension to be 8000 as a good compromise between performance and detectability for efficient steganalysis taking $T = 4$.

2.2. Feature Transformation and Dimensionality Reduction

Dimensionality reduction generally transforms high dimensional features (e.g., 8000 dimensional DCTR features) to lower dimensional ones to avoid overfitting, and helps to avoid various complications arising from the "curse of dimensionality", including overfitting. PCA is a linear method of feature transformation as well as dimensionality reduction, such that the variance of the lower dimensional feature space is maximized [19]. We have incorporated PCA based feature transformation and dimensionality reduction to make the DCTR feature datapoints decorrelated by maximizing the variance among them, thereby enabling efficient machine learning based model building. Selection of the number of principal components is an important optimization decision. For that purpose, we have used the computationally efficient "Modified 95% Variance Method" [20], as follows. A *Singular Value Decomposition* (SVD) of the covariance matrix of the datapoints is performed, and the count "k" is determined such that the largest k singular values $s_{11}, s_{22}, \cdots s_{kk}$ satisfy $\sum_{i=1}^{k} s_{ii} \geq 0.95 \sum_{i=1}^{m} s_{ii}$, where m is the original dimension of the features, and $S = [s_{ij}]$ denotes the singular value matrix after singular value decomposition of the covariance matrix of the feature set. This value of k denotes the number of principal components to be selected such that among the datapoints 95% variance is retained, Our experimental results show that PCA significantly improves the classification accuracy of our experiments by 4-5%.

2.3. Random Forest based Ensemble Classifier

After feature extraction, we used *Random Forest* based multi-class ensemble classifier [21], with decision tree as base learner. There are mainly two well-known techniques for ensemble classification: (a) *Bagging*, and, (b) *Boosting*. Random Forest classifier has several advantages [21], some of which include computational efficiency, ability to represent non-linear decision boundaries, integrated feature selection and classification, and noise resilience. In *Bagging* or *Bootstrap Aggregating* [22], the original training data is first randomly sampled with replacement (i.e., bootstrap sampling). Subsequently, each sample is used to fit a separate base classifier, and finally the base classifiers are combined by taking majority voting or aggregation of the predictions from each base classifier. Bagging reduces variance and also avoids overfitting. *Random Forest* is an extension of Bagging [22], where the decision tree is taken as base classifier, and the prediction of the ensemble classifier is obtained by majority voting among the base classifiers.

Table 1. Camera Models Used in Experiments

Camera ID	Number of Image	Camera Model
1	979	Canon
2	1040	Olympus
3	1331	Samsung
4	1671	Sony
5	1000	Agfa
6	925	Casio
7	630	FujiFilm
8	1000	Kodak
9	1000	Nikon
10	931	Panasonic

Additionally, feature selection is carried out at each node while constructing the decision tree.

Boosting is a weighted ensemble classifier, where each base classifier is assigned a non-negative weight according to its stand-alone classification accuracy [23]. This approach generates a strong classifier by combining several weak base classifiers, termed as "weak learners". The most popular representation of boosting is *AdaBoost* [23]. Classically, AdaBoost was designed for binary classification; however, it is generalized for multiclass classification as *AdaBoost.M1* [23]. We have used the AdaBoost ensemble classifier with Random Forest (itself an ensemble classifier) as the weak learner for training in our source identification framework. Fig. 2 shows the flowchart of the overall framework.

3. Experimental Results

3.1. Experimental Setup

We experimented with 10,507 images taken from 10 camera models as shown in Table 1 from the standard benchmark *Dresden Image Database* [24] (termed as **Dataset-1**). Around 630-1671 images were taken from each camera, aiming to make the experimental database large and hopefully resistant to overfitting. Next, our goal is to identify the camera brand attribute of the images. The colored JPEG images were converted into grayscale images, and DCTR features are calculated with quality factor $Q = 75$. The authors in [11] used their own image dataset for experiments which is not available publicly. Hence, for fair comparison with other state-of-the-art techniques, we evaluated the effectiveness of our approach using a reduced subset of 100 images from each of the 10 camera models from the Dresden Image Database (termed as **Dataset-2**). Note that dataset-1 is used for camera brand attribute identification (i.e., in general camera brand identification) and dataset-2 is used for camera model attribute identification (i.e., specific camera model identification). Experimental result shows that our technique is effective for both the camera brand attribute identification as well as particular camera model attribute identification. We trained the random forest (RF) classifier, with decision tree as base learner using the features and labels (camera model it originally belongs to) given for images in the training set. In our experiments, we used 100 decision trees in the random forest classifier. In this case for AdaBoost, the number of weak learners was taken to be 50 and the learning rate is 1, i.e., the ensemble learns at the maximum possible rate. We have divided the dataset randomly into approximately equal 10 parts, then 9 parts are used for training and the remaining part is used for testing. This is repeated for the 10 different parts individually, and the average accuracy is reported. We also evaluated the classification accuracy for the commonly used *Support Vector Machine* (SVM) classification technique, with *Radial Basis Function* (RBF) kernel.

Table 2. **Comparison of Accuracy for Various Classification Schemes based on DCTR Features (dataset-1)**

Experiment	**Classification Accuracy**
SVM Classifier (RBF kernel)	81.1%
AdaBoost (100 decision trees as weak learner)	45.2%
Random Forest (RF) (100 decision trees as base learner)	93.8%
RF + PCA (168 dim. features)	98.9%
AdaBoost (RF as weak learner) + PCA (168 dim. features)	**99.1%**

We used MATLAB (v. R2015a) in our experiments, and the experiments were run on an iMac workstation with a 3.2 GHz Intel CPU and 8 GB of main memory. The code for feature extraction was adapted from [25]. The *Weka Machine Learning Toolbox* [26] was used for the machine learning based model building and validation experiments.

3.2. Classification Accuracy Improvement (Dataset-1)

The classification accuracy results are summarized in Table 2. We obtained the following classification accuracy results for the DCTR feature sets extracted (we explicitly mention whether dimensionality reduction was used):

- With SVM classification (using RBF kernel) and no dimensionality reduction, the classification accuracy was 81.1%.

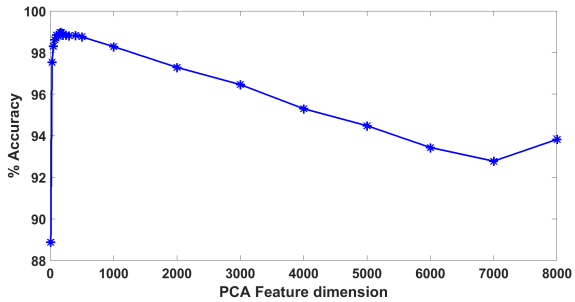

Figure 3. Classification accuracy vs. PCA dimension plot. Accuracy is maximized when PCA dimension is 168.

Table 3. **Confusion Matrix for Proposed Classification Scheme**

Classification Accuracy		**True Model**									
		1	2	3	4	5	6	7	8	9	10
Identified Model	1	**98.8**	0	0.2	0	0.6	0.1	0	0	0.3	0
	2	0	**99.8**	0	0	0.1	0	0	0	0.1	0
	3	0.2	0.1	**98.9**	0	0.5	0	0	0	0.2	0.1
	4	0	0	0	**99.8**	0.2	0	0	0	0	0
	5	0.3	0	0.8	0.4	**96.9**	0.4	0	0.1	1.0	0.1
	6	0.1	0	0	0.1	0.1	**99.7**	0	0	0	0
	7	0.2	0	0	0	0.1	0	**99.5**	0	0.2	0
	8	0.1	0	0	0	0.1	0	0	**99.8**	0	0
	9	0.2	0	0	0	1.6	0	0	0.1	**98.1**	0
	10	0	0	0.1	0	0.2	0	0	0	0.2	**99.5**

Table 4. **Accuracy Comparison with State-of-the-art Techniques (Dataset-2)**

Approach	**Classification Accuracy**
Co-occurrence matrix feature [11] + RF	80.1%
Co-occurrence matrix feature [11] + RF + PCA (100 dim. features)	90.3%
Co-occurrence matrix feature [11] + RF + PCA (100 dim. features) + AdaBoost	91.4%
Co-occurrence matrix feature + FLD (approach of [11])	95.8%
DCTR Feature + SFFS [27]	75.3%
DCTR Feature + RF	81.9%
DCTR Feature + RF + AdaBoost	83.4%
DCTR Feature + FLD	95.6%
DCTR Feature + PCA (130 dim. features) + FLD	96.2%
DCTR Feature + RF + PCA (130 dim. features)	96.3%
DCTR Feature + RF + PCA (130 dim. features) + AdaBoost	**96.5%**

- For AdaBoost based ensemble classifier with 100 decision trees as weak learner, and no dimensionality reduction, we obtained only 45.2% accuracy.

- For Random Forest (RF) classification, with decision tree as base learner and no dimensionality reduction, we got an average classification accuracy of 93.8%.

- RF classifier, in conjunction with PCA based dimensionality reduction, enables us to reach a classification accuracy of 98.9%. The optimal dimensionality was detecrmined by the "Modified 95% Variance" method to be 168, as depicted in Fig. 3.

- Finally, when we use *AdaBoost* with RF as weak learner, combined with PCA for dimensionality reduction, the classification accuracy improves to **99.1%**. The corresponding confusion matrix for the the 10-class camera source classification problem is shown in Table 3.

3.3. Comparison of Accuracy with State-of-the-Art Techniques (Dataset-2)

We have compared our approach with different state-of-the-art approach reported in [11] using co-occurrence based *Spatial and Color Rich Model with Fixed Quantization* $q = 1$ (SRMQ1) for Dataset-2. For both the cases, the extracted features were used to train the same RF classifier (with number of trees being 100). The resulting classification accuracy figures have been presented in Table 4, whereby we find that our proposed approach is more effective than the state-of-the-art co-occurrence matrix based feature approach [11], with respect to the same RF based classifier. The accuracy reached by our proposed DCTR feature based approach (when both PCA and AdaBoost are used) is still superior when we experimented with the multi-class ensemble classifier using *Fisher Linear Discriminant* (FLD) based binary classifiers proposed in [11]. Moreover, as dataset-2 is to be considered for particular camera model identification, we observe that our technique is also quite efficient identifying particular camera models.

Along with the accuracy improvement with respect to the choice of features, we also compared with other dimensionality reduction techniques. When we applied the *Subset Size Feature Selection* (SFFS) technique to select the features [27], we found that it is not very effective, as shown by the accuracy results in Table 4. This can be explained to be happening probably because the feature dimensions (8,000 for DCTR) are too large for SFFS to be effective. However, PCA based dimensionality reduction (which reduces feature dimension from 8000 to 130 for Dataset-2) improves the accuracy significantly as shown in Table 4, especially when AdaBoost is applied.

3.4. Evaluation of Overfitting Trends

To evaluate the robustness to overfitting, we took the classifier (DCTR + PCA (168) + RF (number of trees = 100) + AdaBoost) built using Dataset-1, and then evaluated the accuracy for **images from a completely different *Sensor Dust Image Dataset*** [28], for two camera models: *Kodak-M1063* and *Canon-Ixus55*. The average accuracy obtained was 97.08%, which demonstrates that the classification model built has good generalization capability, and is not prone to overfitting.

4. Conclusion

We have proposed and developed a DCTR feature based source camera identification framework, with random forest based ensemble classification fortified by AdaBoost. The DCTR features effectively capture the JPEG compression artifacts imposed on the image by the quantization table used for JPEG compression by image camera source. PCA based dimensionality reduction of the features prior to classification model building improves the classification accuracy. Our technique outperforms other state-of-the-art techniques when applied on a large benchmark image dataset from 10 different camera sources, and demonstrates low overfitting trends.

Acknowledgement

This research was supported by Research Grant No. SB/FTP/ETA-0191/2013 from *Science and Engineering Research Board* (SERB), Govt. of India.

References

[1] M. Kharrazi, H. T. Sencar, and N. Memon, "Blind source camera identification," in *International Conference on Image Processing, 2004. ICIP'04. 2004*, vol. 1. IEEE, 2004, pp. 709–712. 1

[2] A. Swaminathan, M. Wu, and K. R. Liu, "Nonintrusive component forensics of visual sensors using output images," *IEEE Transactions on Information Forensics and Security*, vol. 2, no. 1, pp. 91–106, 2007. 1

[3] H. Cao and A. C. Kot, "Accurate detection of demosaicing regularity for digital image forensics," *IEEE Transactions on Information Forensics and Security*, vol. 4, no. 4, pp. 899–910, 2009. 1

[4] T. Filler, J. Fridrich, and M. Goljan, "Using sensor pattern noise for camera model identification," in *15th IEEE International Conference on Image Processing*. IEEE, 2008, pp. 1296–1299. 1

[5] L. T. Van, S. Emmanuel, and M. S. Kankanhalli, "Identifying source cell phone using chromatic aberration," in *IEEE International Conference on Multimedia and Expo*. IEEE, 2007, pp. 883–886. 1

[6] E. Kee, M. K. Johnson, and H. Farid, "Digital image authentication from jpeg headers," *IEEE Transactions on Information Forensics and Security*, vol. 6, no. 3, pp. 1066–1075, 2011. 1

[7] K. San Choi, E. Y. Lam, and K. K. Wong, "Source camera identification using footprints from lens aberration," in *Electronic Imaging 2006*. International Society for Optics and Photonics, 2006, pp. 60 690J–60 690J. 1

[8] A. E. Dirik, H. T. Sencar, and N. Memon, "Source camera identification based on sensor dust characteristics," in *Signal Processing Applications for Public Security and Forensics, 2007. SAFE'07. IEEE Workshop on*. IEEE, 2007, pp. 1–6. 1

[9] S. Bayram, H. T. Sencar, N. Memon, and I. Avcibas, "Improvements on source camera-model identification based on cfa interpolation," *Proc. of WG*, vol. 11, pp. 24–27, 2006. 1

[10] G. Xu and Y. Q. Shi, "Camera model identification using local binary patterns," in *International Conference on Multimedia and Expo (ICME), 2012 IEEE*. IEEE, 2012, pp. 392–397. 1

[11] C. Chen and M. C. Stamm, "Camera model identification framework using an ensemble of demosaicing features," in *IEEE International Workshop on Information Forensics and Security (WIFS), 2015*. IEEE, 2015, pp. 1–6. 1, 4, 5

[12] J. Fridrich and J. Kodovsky, "Rich models for steganalysis of digital images," *IEEE Transactions on Information Forensics and Security*, vol. 7, no. 3, pp. 868–882, 2012. 1

[13] F. Marra, G. Poggi, C. Sansone, and L. Verdoliva, "A study of co-occurrence based local features for camera model identification," *Multimedia Tools and Applications*, pp. 1–17, 2016. 1

[14] A. Tuama, F. Comby, and M. Chaumont, "Source camera model identification using features from contaminated sensor noise," in *International Workshop on Digital Watermarking*. Springer, 2015, pp. 83–93. 1

[15] ——, "Camera model identification based machine learning approach with high order statistics features," in *European Signal Processing Conference*, 2016, pp. 1183–1187. 1

[16] R. C. Gonzalez and R. E. Woods, *Digital Image Processing (3rd ed.)*. Prentice Hall, 2008. 1

[17] V. Holub and J. Fridrich, "Low-complexity features for jpeg steganalysis using undecimated dct," *IEEE Transactions on Information Forensics and Security*, vol. 10, no. 2, pp. 219–228, 2015. 1, 2, 3

[18] X. Song, F. Liu, C. Yang, X. Luo, and Y. Zhang, "Steganalysis of adaptive jpeg steganography using 2d gabor filters," in *Proceedings of the 3rd ACM Workshop on Information Hiding and Multimedia Security*. ACM, 2015, pp. 15–23. 2

[19] R. O. Duda, P. E. Hart, and D. G. Stork, *Pattern Classification*. John Wiley and Sons, 2012. 3

[20] A. Ng, "Machine learning," https://www.coursera.org/learn/machine-learning. 3

[21] A. Criminisi, J. Shotton, and E. Konukoglu, "Decision forests for classification, regression, density estimation, manifold learning and semi-supervised learning," *Microsoft Research Cambridge, Tech. Rep. MSRTR-2011-114*, vol. 5, no. 6, p. 12, 2011. 3

[22] O. Okun, *Feature selection and ensemble methods for bioinformatics: algorithmic classification and implementations*. Medical Information Science Reference, 2011. 3

[23] Y. Freund, R. E. Schapire *et al.*, "Experiments with a new boosting algorithm," in *ICML*, vol. 96, 1996, pp. 148–156. 4

[24] T. Gloe and R. Böhme, "The dresden image database for benchmarking digital image forensics," *Journal of Digital Forensic Practice*, vol. 3, no. 2-4, pp. 150–159, 2010. 4

[25] "Feature extractors for steganalysis," http://dde.binghamton.edu/download/feature_extractors/. 4

[26] M. Hall, E. Frank, G. Holmes, B. Pfahringer, P. Reutemann, and I. H. Witten, "The weka data mining software: an update," *ACM SIGKDD explorations newsletter*, vol. 11, no. 1, pp. 10–18, 2009. 4

[27] O. Çeliktutan, B. Sankur, and I. Avcibas, "Blind identification of source cell-phone model." *IEEE Transactions on Information Forensics and Security*, vol. 3, no. 3, pp. 553–566, 2008. 5

[28] "Sensor Dust Image Dataset," http://isis.poly.edu/~emir/sensordust/sensordust3.html. 6